
Temporally Disentangled Representation Learning under Unknown Nonstationarity

Xiangchen Song^{1*} Weiran Yao² Yewen Fan¹ Xinshuai Dong¹ Guangyi Chen^{1,3}
Juan Carlos Niebles² Eric Xing^{1,3} Kun Zhang^{1,3}

¹Carnegie Mellon University

²Salesforce Research

³Mohamed bin Zayed University of Artificial Intelligence

Abstract

In unsupervised causal representation learning for sequential data with time-delayed latent causal influences, strong identifiability results for the disentanglement of causally-related latent variables have been established in stationary settings by leveraging temporal structure. However, in *nonstationary* setting, existing work only partially addressed the problem by either utilizing observed auxiliary variables (e.g., class labels and/or domain indexes) as side-information or assuming simplified latent causal dynamics. Both constrain the method to a limited range of scenarios. In this study, we further explored the Markov Assumption under time-delayed causally related process in *nonstationary* setting and showed that under mild conditions, the independent latent components can be recovered from their nonlinear mixture up to a permutation and a component-wise transformation, *without* the observation of auxiliary variables. We then introduce NCTRL, a principled estimation framework, to reconstruct time-delayed latent causal variables and identify their relations from measured sequential data only. Empirical evaluations demonstrated the reliable identification of time-delayed latent causal influences, with our methodology substantially outperforming existing baselines that fail to exploit the nonstationarity adequately and then, consequently, cannot distinguish distribution shifts.

1 Introduction

Causal reasoning for time-series data is a long-lasting yet fundamental task [1–3]. The majority of the studies focus on the temporal causal discovery among observed variables [4–6]. However, in many real-world scenarios, the observed data (e.g., image pixels in videos) instead of having direct causal edges, are generated by some causally related latent temporal processes or confounders. Learning causal relations has practical use cases, which benefit a lot of downstream tasks. However, estimating latent causal structures among those unobserved variables purely from observations without appropriate class of assumptions is an extremely challenging task (i.e. the latent variables are generally not identifiable) [7, 8].

Under the topic of unsupervised representation learning via nonlinear Independent Component Analysis (ICA), some strong identifiability results of the latent variables have been established [9–14] by introducing side information such as class labels and domain indices. Specifically focusing on time-series data, history information is also widely used as the side information for the identifiability of latent processes [15–18]. However, existing studies mainly focused on and derived identifiability results in stationary settings [10, 16] (Fig 1a) or nonstationary settings with explicitly observed domain indices [12, 17, 18] (Fig 1b).

*Part of the work was done while interning at Salesforce Research

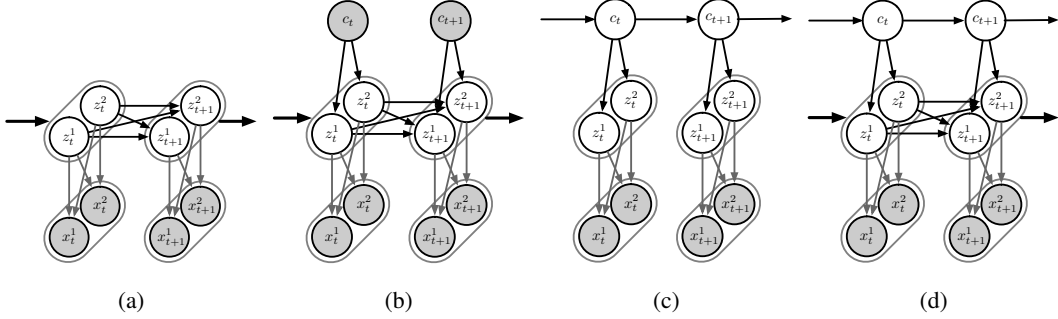


Figure 1: Graphical models for different settings in causally related time-delayed time-series data with a visual illustration. (a) is a *stationary* setting in which the transition function $\mathbf{z}_{t+1} = f_z(\mathbf{z}_t)$ remains universally the same. (b) is the setting widely explored in existing work, in which the transition function f_z changes according to different domains (denoted as c_t), and all these domain indices are observed. (c) capture the unobserved domain indices by introducing a Markov chain on c_t . (d) is a more general form to model the time-series data in this work. It allows nonstationary settings and it does not require the domain indices to be observed. In all cases, the mapping from \mathbf{z}_t to \mathbf{x}_t is deterministic, which is indicated by a gray arrow.

One can immediately tell the infeasibility of those two scenarios that general time-series data is usually nonstationary and the side information (class labels and domain indices) is usually unobserved. That is particularly true when considering real-world data such as video or signal sequences. It doesn't make any sense to assume that there exists a stationary transition function that is applied to the whole video clip. Take a very simple video clip of a mouse² [19] as an example, it is fairly clear that such a simple motion example can be divided into at least two phases (1) active phase in which the mouse is moving and (2) inactive phase in which the mouse is laying down. Instead of using a complex transition function to describe the whole video clip, a more reasonable assumption is that the same transition function is shared within the same phase, but across different phases, the transition functions are different, in other words, the transition function can be expressed as a function of the domain index. Also, it is worth mentioning that if such domain or phase indices is latent or unobserved, then we cannot directly utilize the existing framework to learn the latent causal dynamics. That is again a more realistic case that in general, the domain indices within a video are not accessible without expensive human annotation.

Recently, HMNLICA [14] attempted to resolve the problem by introducing Markov Assumption on the nonstationary discrete domain variable, they assumed the domain indices follow a first-order Markov Chain and estimated the domain information purely from observed data. However, HMNLICA assumes temporally mutually independent sources in the data-generating process (conditioning on domain indices), i.e. they don't allow latent variables to have time-delayed causal relations in between (Fig 1c). Such an assumption imposed a huge negative impact on the usability of those methods. Considering the video of the little mouse example, the \mathbf{x}_t s are the observed video frames, \mathbf{z}_t s can be the independent motion dynamics or causal process such as position, velocity, (angular) momentum, etc, and c_t s are the phases or actions such as standing up (active) and laying down (inactive). To accommodate for such general sequential data, time-delayed temporal dependence should be considered in the latent \mathbf{z}_t space (Fig 1d, otherwise, it is impossible to model a complex video data's temporal relation purely from discrete, domain indices. Also to make sure that the latent independent components can be recovered, temporally conditional independence should also be enforced, i.e. Each dimension of \mathbf{z}_t is conditionally independent given the history $\mathbf{z}_{\text{history}}$. To this end, a natural question is:

How can we establish identifiability of nonlinear ICA for general sequential data with nonstationary causally-related process without observing auxiliary variable?

To answer this question, we first formulate the latent nonstationary states as a discrete Markov process and further explore the Markov Assumption [20] which is introduced for identifiability of nonlinear ICA in HMNLICA [14] and use stronger identifiability result corresponding to the conditional

²<https://dattalab.github.io/moseq2-website/images/sample-extraction.gif>.

emission distribution (i.e. the transition function of different domains) and the transition matrix of the Markov process. Specifically, we leverage the identifiability of Autoregressive Hidden Markov Models in [21] to accommodate time-delayed causally-related non-parametric transitions in latent space. Then we utilize the linear independence (Thm. 2) to further establish the identifiability of \mathbf{z}_t .

The main contributions of this work can be summarized as follows:

- To our best knowledge, this is the first identifiability result that can handle the nonstationary time-delayed causally-related latent temporal processes without the auxiliary variable. We formulate the problem, especially the nonstationary states into the Markov process, establish identifiability purely from observed data, and then show strong identifiability of latent independent components.
- We present **NCTRL**, **Nonstationary Causal Temporal Representation Learning**, a principled framework to recover time-delayed latent causal variables and identify their relations from measured sequential data under unobserved different distribution shifts.
- Experiments on both synthetic and real-world datasets demonstrate the effectiveness of the proposed method in recovering the latent variables.

2 Problem Formulation

2.1 Time Series Generative Model

Assume we observe m -dimensional time-series data at discrete time steps, $\mathbf{X} = \{\mathbf{x}_1, \mathbf{x}_2, \dots, \mathbf{x}_T\}$, where each $\mathbf{x}_t \in \mathbb{R}^m$ is generated from time-delayed causally related hidden components $\mathbf{z}_t \in \mathbb{R}^n$ by the invertible mixing function:

$$\mathbf{x}_t = \mathbf{g}(\mathbf{z}_t). \quad (1)$$

In addition to latent components \mathbf{z}_t , there is an extra hidden variable c_t which is discrete with cardinality $|c_t| = C$, it follows a first-order Markov process controlled by a $C \times C$ transition matrix \mathbf{A} , in which the i, j -th entry $A_{i,j}$ is the probability to transit from state i to j .

$$c_1, c_2, \dots, c_t \sim \text{Markov Chain}(\mathbf{A}) \quad (2)$$

For $i \in \{1, \dots, n\}$, z_{it} , as the i -th component of \mathbf{z}_t , is generated by (some) components of history information \mathbf{z}_{t-1} , discrete nonstationary indicator c_t , and noise ϵ_{it} ³.

$$z_{it} = f_i(\{z_{j,t-1} \mid z_{j,t-\tau} \in \mathbf{Pa}(z_{it})\}, c_t, \epsilon_{it}) \quad \text{with} \quad \epsilon_{it} \sim p_{\epsilon_i} \quad (3)$$

where $\mathbf{Pa}(z_{it})$ is the set of latent factors that directly cause z_{it} , which can be any subset of $\mathbf{z}_{\text{HX}} = \{\mathbf{z}_{t-1}, \mathbf{z}_{t-2}, \dots, \mathbf{z}_{t-L}\}$ up to history information maximum lag L . The components of \mathbf{z}_t are mutually independent conditional on \mathbf{z}_{HX} and c_t .

2.2 Identifiability of Latent Causal Processes and Time-Delayed Latent Causal Relations

We define the identifiability of time-delayed latent causal processes in the representation function space in **Definition 1**. Furthermore, if the estimated latent processes can be identified at least up to permutation and component-wise invertible nonlinearities, the latent causal relations are also immediately identifiable because conditional independence relations fully characterize time-delayed causal relations in a time-delayed causally sufficient system, in which there are no latent causal confounders in the (latent) causal processes. Note that invertible component-wise transformations on latent causal processes do not change their conditional independence relations.

Definition 1 (Identifiable Latent Causal Processes). *Formally let $\mathbf{X} = \{\mathbf{x}_1, \mathbf{x}_2, \dots, \mathbf{x}_T\}$ be a sequence of observed variables generated by the true temporally causal latent processes specified by $(f_i, p(\epsilon_i), \mathbf{A}, \mathbf{g})$ given in Eqs. (1), (2), and (3). A learned generative model $(\hat{f}_i, \hat{p}(\epsilon_i), \hat{\mathbf{A}}, \hat{\mathbf{g}})$ is observationally equivalent to $(f_i, p(\epsilon_i), \mathbf{A}, \mathbf{g})$ if the model distribution $p_{\hat{g}, \hat{p}, \hat{\mathbf{A}}, \hat{\mathbf{g}}}(\{\mathbf{x}_1, \mathbf{x}_2, \dots, \mathbf{x}_T\})$*

³Here for different values of c_t the corresponding transition functions f_i are not identical. Otherwise the states can be merged.

matches the data distribution $p_{f_i, p_{\epsilon_i}, \mathbf{A}, \mathbf{g}}(\{\mathbf{x}_1, \mathbf{x}_2, \dots, \mathbf{x}_T\})$ everywhere. We say latent causal processes are identifiable if observational equivalence can lead to identifiability of the latent variables up to permutation π and component-wise invertible transformation T :

$$\begin{aligned} p_{\hat{f}_i, \hat{p}_{\epsilon_i}, \hat{\mathbf{A}}, \hat{\mathbf{g}}}(\{\mathbf{x}_1, \mathbf{x}_2, \dots, \mathbf{x}_T\}) &= p_{f_i, p_{\epsilon_i}, \mathbf{A}, \mathbf{g}}(\{\mathbf{x}_1, \mathbf{x}_2, \dots, \mathbf{x}_T\}) \\ \Rightarrow \hat{\mathbf{g}}^{-1}(\mathbf{x}_t) &= T \circ \pi \circ \mathbf{g}^{-1}(\mathbf{x}_t), \quad \forall \mathbf{x}_t \in \mathcal{X}, \end{aligned} \quad (4)$$

where \mathcal{X} is the observation space.

3 Identifiability Theory

In this section, we showed that under mild conditions, the latent variable \mathbf{z}_t is identifiable up to permutation and a component-wise transformation. The theoretical results can be divided into two parts (1) identifiability of the nonstationarity and (2) identifiability of the independent components. As introduced above, the major challenge comes from the unobserved domain indices or nonstationary indicators (c_t in our graphic models). We leverage the identifiability of the different conditional distributions from the observed data and then show that the latent variables \mathbf{z} are identifiable. Complete proofs can be found in Appendix A.

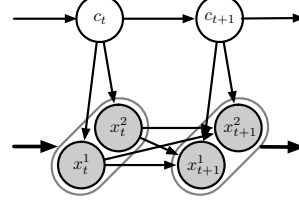


Figure 2: Graphical model used in Lemma 1, which only considers c_t and \mathbf{x}_t .

3.1 Identifiability of Nonstationary Hidden States

We first introduce a lemma from [21], which established identifiability of Markov switching models, and then we argue that under some mild assumptions on the data generating process, the Markov switching part of our model is also identifiable.

The family of first-order MSMs can be expressed in a finite mixture model form as follows:

$$\mathcal{M}^T := \left\{ \sum_{c_{1:T}} p(c_{1:T}) p_{c_1}(\mathbf{x}_1) \prod_{t=2}^T p(\mathbf{x}_t | \mathbf{x}_{t-1}, c_t) \mid |\mathcal{C}| < +\infty, t \geq 2, c_t \in \mathcal{C}, \sum_{c_{1:T}} p(c_{1:T}) = 1 \right\}. \quad (5)$$

And the identifiability of this model is defined as follows:

Definition 2 (Definition 3.1 in [21]). *The first-order Markov switching model family \mathcal{M}^T is said to be identifiable up to permutations, when for $p(\mathbf{x}_1, \mathbf{x}_2, \dots, \mathbf{x}_T) = \hat{p}(\mathbf{x}_1, \mathbf{x}_2, \dots, \mathbf{x}_T), \forall \mathbf{x}_1, \mathbf{x}_2, \dots, \mathbf{x}_T \in \mathbb{R}^{Tm}$, if and only if $|\mathcal{C}| = |\hat{\mathcal{C}}|$ and for each $c_{1:T}$ there is some $\hat{c}_{1:T}$ s.t.*

1. $p(c_{1:T}) = \hat{p}(\hat{c}_{1:T});$
2. if $c_{t_1} = c_{t_2}$ for $t_1, t_2 \geq 2$ and $t_1 \neq t_2$, then $\hat{c}_{t_1} = \hat{c}_{t_2};$
3. $p(\mathbf{x}_t | \mathbf{x}_{t-1}, c_t) = \hat{p}(\mathbf{x}_t | \mathbf{x}_{t-1}, \hat{c}_t), \forall t \geq 2, \mathbf{x}_t, \mathbf{x}_{t-1} \in \mathbb{R}^m;$
4. $p_{c_1}(\mathbf{x}_1) = p_{\hat{c}_1}(\mathbf{x}_1), \forall \mathbf{x}_1 \in \mathbb{R}^m.$

Then Balsells-Rodas et al.[21] showed if the transition and initial distribution is in Gaussian family with unique indexing, the model is identifiable.

Lemma 1. (Theorem 3.1 in [21]) *Define the following first-order Markov switching model family under non-linear Gaussian families with the following assumptions held:*

i *The transition is in a non-linear Gaussian family with unique indexing:*

$$\begin{aligned} \mathcal{G}_{\mathcal{C}} &= \{p(\mathbf{x}_t | \mathbf{x}_{t-1}, c) = \mathcal{N}(\mathbf{m}(\mathbf{x}_{t-1}, c), \Sigma(\mathbf{x}_{t-1}, c)) \mid c \in \mathcal{C}, \mathbf{x}_t, \mathbf{x}_{t-1} \in \mathbb{R}^m\}, \\ \forall c \neq c' \in \mathcal{C}, \exists \mathbf{x}_{t-1} \in \mathbb{R}^m, \text{ s.t. } \mathbf{m}(\mathbf{x}_{t-1}, c) &\neq \mathbf{m}(\mathbf{x}_{t-1}, c') \text{ or } \Sigma(\mathbf{x}_{t-1}, c) \neq \Sigma(\mathbf{x}_{t-1}, c'). \end{aligned}$$

ii *Also for initial distributions:*

$$\begin{aligned} \mathcal{I}_{\mathcal{C}} &:= \{p(\mathbf{x}_1 | c) = \mathcal{N}(\boldsymbol{\mu}(c), \Sigma_1(c)) \mid c \in \mathcal{C}\}, \\ c \neq c' \in \mathcal{C} &\Leftrightarrow \boldsymbol{\mu}(c) \neq \boldsymbol{\mu}(c') \text{ or } \Sigma_1(c) \neq \Sigma_1(c'). \end{aligned}$$

iii *For any $c \in \mathcal{C}$, the mean and covariance, $\mathbf{m}(\cdot, c) : \mathbb{R}^m \rightarrow \mathbb{R}^m$ and $\Sigma(\cdot, c) : \mathbb{R}^m \rightarrow \mathbb{R}^{m \times m}$, are analytic functions.*

where $\mathbf{m}(\mathbf{x}_{t-1}, c)$ and $\Sigma(\mathbf{x}_{t-1}, c)$ are non-linear with respect to \mathbf{z}_{t-1} and denote the mean and covariance matrix of the Gaussian distribution, and \mathcal{C} is an index set satisfying mild measure-theoretic conditions. Then the Markov switching model is identifiable in terms of Def. 2.

Definition 3 (volume-preserving mapping). A mapping $f : \mathcal{A} \rightarrow \mathcal{B}$ is said to be volume-preserving if

$$|\mathbf{J}_f(a)| = 1, \quad \forall a \in \mathcal{A}.$$

Theorem 1 (identifiability of nonstationary hidden states). Suppose the observed data is generated following the nonlinear ICA framework as defined in Eqs. (1), (2) and (3). And suppose the following assumptions hold:

- i The mixing function in Eq. (1) and its inverse are analytic and preserve volume (Def. 3).
- ii The transition in Eq. (3) is in Gaussian family, and the transition functions f_i are analytic.

Then the Markov switching model is identifiable in terms of Def. 2.

Furthermore, Corollary 3.1 in [21] further shows that the parameters of the Markov chain $p(c_{t+1} | c_t)$ and $p(c_1)$ are identifiable up to permutations, providing a mapping $\hat{c} = \sigma(c)$.

For notational simplicity and without loss of generality, we can assume that the states are ordered such that $c = \sigma(c)$. This provides us with a bridge to further leverage the temporal independence condition in the latent space to establish the identifiability result for the demixing function or, in other words, the latent variables \mathbf{z}_t .

3.2 Identifiability of Latent Causal Processes

To incorporate non-linear ICA into the Markov switching model, we define the emission distribution $p(\mathbf{x}_t | \mathbf{x}_{t-1}, c)$ as a deep latent variable model. First, the latent independent component variables $\mathbf{z}_t \in \mathbb{R}^n$ are generated from a factorial prior, given the hidden state c_t and the previous \mathbf{z}_{t-1} , as

$$p(\mathbf{z}_t | \mathbf{z}_{t-1}, c_t) = \prod_{k=1}^n p(z_{kt} | \mathbf{z}_{t-1}, c_t). \quad (6)$$

Second, the observed \mathbf{x}_t is generated by a non-linear mixing function as in Eq. (1) which is assumed to be bijective with inverse given by $\mathbf{z}_t = \mathbf{g}(\mathbf{x}_t)$. Let $\eta_{kt}(c_t) \triangleq \log p(z_{kt} | \mathbf{z}_{t-1}, c_t)$, and assume that $\eta_{kt}(c_t)$ is twice differentiable in z_{kt} and is differentiable in $z_{l,t-1}$, $l = 1, 2, \dots, n$. Note that the parents of z_{kt} may be only c_t and a subset of \mathbf{z}_{t-1} ; if $z_{l,t-1}$ is not a parent of z_{kt} , then $\frac{\partial \eta_{kt}}{\partial z_{l,t-1}} = 0$.

Theorem 2. (identifiability of the independent components) Suppose there exists an invertible function $\hat{\mathbf{g}}^{-1}$, which is the estimated demixing function that maps \mathbf{x}_t to $\hat{\mathbf{z}}_t$, i.e.,

$$\hat{\mathbf{z}}_t = \hat{\mathbf{g}}^{-1}(\mathbf{x}_t) \quad (7)$$

such that the components of $\hat{\mathbf{z}}_t$ are mutually independent conditional on $\hat{\mathbf{z}}_{t-1}$. Let

$$\begin{aligned} \mathbf{v}_{k,t}(c) &\triangleq \left(\frac{\partial^2 \eta_{kt}(c)}{\partial z_{k,t} \partial z_{1,t-1}}, \frac{\partial^2 \eta_{kt}(c)}{\partial z_{k,t} \partial z_{2,t-1}}, \dots, \frac{\partial^2 \eta_{kt}(c)}{\partial z_{k,t} \partial z_{n,t-1}} \right)^\top, \\ \hat{\mathbf{v}}_{k,t}(c) &\triangleq \left(\frac{\partial^3 \eta_{kt}(c)}{\partial z_{k,t}^2 \partial z_{1,t-1}}, \frac{\partial^3 \eta_{kt}(c)}{\partial z_{k,t}^2 \partial z_{2,t-1}}, \dots, \frac{\partial^3 \eta_{kt}(c)}{\partial z_{k,t}^2 \partial z_{n,t-1}} \right)^\top. \end{aligned} \quad (8)$$

And

$$\begin{aligned} \mathbf{s}_{kt} &\triangleq \left(\mathbf{v}_{kt}(1)^\top, \dots, \mathbf{v}_{kt}(C)^\top, \frac{\partial^2 \eta_{kt}(2)}{\partial z_{kt}^2} - \frac{\partial^2 \eta_{kt}(1)}{\partial z_{kt}^2}, \dots, \frac{\partial^2 \eta_{kt}(C)}{\partial z_{kt}^2} - \frac{\partial^2 \eta_{kt}(C-1)}{\partial z_{kt}^2} \right)^\top, \\ \hat{\mathbf{s}}_{kt} &\triangleq \left(\hat{\mathbf{v}}_{kt}(1)^\top, \dots, \hat{\mathbf{v}}_{kt}(C)^\top, \frac{\partial \eta_{kt}(2)}{\partial z_{kt}} - \frac{\partial \eta_{kt}(1)}{\partial z_{kt}}, \dots, \frac{\partial \eta_{kt}(C)}{\partial z_{kt}} - \frac{\partial \eta_{kt}(C-1)}{\partial z_{kt}} \right)^\top. \end{aligned} \quad (9)$$

If for each value of \mathbf{z}_t , $\mathbf{s}_{1t}, \hat{\mathbf{s}}_{1t}, \mathbf{v}_{2t}, \hat{\mathbf{s}}_{2t}, \dots, \mathbf{s}_{nt}, \hat{\mathbf{s}}_{nt}$, as $2n$ function vectors $\mathbf{s}_{k,t}$ and $\hat{\mathbf{s}}_{k,t}$, with $k = 1, 2, \dots, n$, are linearly independent, then $\hat{\mathbf{z}}_t$ must be an invertible, component-wise transformation of a permuted version of \mathbf{z}_t .

So far, the identifiability result has been established without observing the nonstationarity indicators such as domain indices. In the next section, a novel variable auto-encoder-based method is introduced to estimate the demixing function $\hat{\mathbf{g}}^{-1}$.

4 NCTRL: Nonstationary Causal Temporal Representation Learning

In this section, we present the details of NCTRL to estimate the latent causal processes under unobserved nonstationary distribution shift, given the identifiability results in Sec. 3. First, we show that our framework includes three modules, Autoregressive Hidden Markov Module, Prior Network, and Encoder-Decoder Module. Then, we provide the optimization objective of our model training including an HMM free-energy lower bound, a reconstruction likelihood loss, and a KL divergence.

4.1 Model Architecture

Our framework extends Sequential Variational Auto-Encoders [22] with tailored modules to model nonstationarity, and enforces the conditions in Sec. 3 as constraints. We give the estimation procedure of the latent causal dynamics model in Eq. (3). The model architecture is shown in Fig. 3. The framework has three major components (1) Autoregressive Hidden Markov Module (ARHMM), (2) Prior Network Module, and (3) Encoder-Decoder Module.

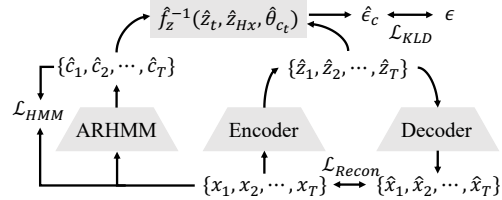


Figure 3: Illustration of NCTRL with (1) Autoregressive Hidden Markov Module, (2) Prior Network, and (3) Encoder-Decoder Module.

Autoregressive Hidden Markov Module (ARHMM) The first component of our framework is ARHMM which deals with the nonstationarity with unobserved domains. As discussed in Thm 1, the transition function or conditional emission distributions across different domains together with the Markov transition matrix \mathbf{A} are identifiable. This module estimates the transition function of different domains $p(\mathbf{x}_t | \mathbf{x}_{t-1}, c_t)$ and the transition matrix \mathbf{A} of the Markov process, and ultimately decodes the optimal domain indices $\{\hat{c}_1, \hat{c}_2, \dots, \hat{c}_T\}$ via the Viterbi algorithm.

Prior Network Module To better estimate the prior distribution $p(\hat{z}_t | \hat{\mathbf{z}}_{\text{HX}}, c_t)$, let \mathbf{z}_{HX} denote the lagged latent variables up to maximum time lag L . We evaluate $p(\hat{z}_t | \hat{\mathbf{z}}_{\text{HX}}, c_t) = p_\epsilon \left(\hat{f}_z^{-1}(\hat{z}_t, \hat{\mathbf{z}}_{\text{HX}}, \hat{\theta}_{c_t}) \right) \left| \frac{\partial \hat{f}_z^{-1}}{\partial \hat{z}_t} \right|$ by learning a holistic inverse dynamics \hat{f}_z^{-1} that takes the estimated change factors for dynamics $\hat{\theta}_{c_t}$ as inputs. The conditional independence of the estimated latent variables $p(\hat{z}_t | \hat{\mathbf{z}}_{\text{HX}})$ is enforced by summing up all estimated component densities when obtaining the joint $p(\mathbf{z}_t | \mathbf{z}_{\text{HX}}, c_t)$ in Eq. 10. Given that the Jacobian is lower-triangular, we can compute its determinant as the product of diagonal terms. The detailed derivations are given in Appendix B.2.

$$\log p(\hat{\mathbf{z}}_t | \hat{\mathbf{z}}_{\text{HX}}, c_t) = \underbrace{\sum_{i=1}^n \log p(\hat{z}_i | c_t)}_{\text{Conditional independence}} + \underbrace{\sum_{i=1}^n \log \left| \frac{\partial \hat{f}_i^{-1}}{\partial \hat{z}_{it}} \right|}_{\text{Lower-triangular Jacobian}} \quad (10)$$

Encoder-Decoder Module The third component is a Variational Auto-Encoder based module which utilizes reconstruction loss to enforce the invertibility of learned mixing function $\hat{\mathbf{g}}$. Specifically, the encoder fits the demixing function $\hat{\mathbf{g}}^{-1}$ and the decoder fits the mixing function $\hat{\mathbf{g}}$. The details of the implementation are in Appendix B.

4.2 Optimization

The first training objective of NCTRL is to maximize the Log-likelihood of the observed data:

$$\log p_{\theta_{\text{HMM}}}(\{\mathbf{x}_1, \mathbf{x}_2, \dots, \mathbf{x}_T\}) \quad (11)$$

where θ_{HMM} represents the HMM training parameters. Then the free energy lower bound can be defined as:

$$-\mathcal{L}_{\text{HMM}} = \mathcal{L}(q(\mathbf{c}), \theta_{\text{HMM}}) \triangleq \mathbb{E}_{q(\mathbf{c})} [\log p_{\theta_{\text{HMM}}}(\mathbf{x}_1, \mathbf{x}_2, \dots, \mathbf{x}_T, \mathbf{c})] - \mathbf{H}(q(\mathbf{c})) \quad (12)$$

Consistent with the theory part, the first training objective is to maximize data log-likelihood in the ARHMM module to get optimal $q(\mathbf{c}^*)$.

$$q(\mathbf{c}^*) \triangleq \arg \max_{q(\mathbf{c})} \mathcal{L}(q(\mathbf{c}), \theta_{\text{HMM}}) \quad (13)$$

which can easily be computed by the Forward-Backward algorithm and luckily all of it is differentiable to the HMM training parameters θ_{HMM} (transition matrix \mathbf{A} and transition function parameters θ_f).

Then the second part is to maximize the Evidence Lower BOund (ELBO) for the VAE framework, which can be written as (complete derivation steps are in Appendix B.3):

$$\begin{aligned} \text{ELBO} &\triangleq \log p_{\text{data}}(\mathbf{X}) - D_{KL}(q_{\phi}(\mathbf{Z}|\mathbf{X})||p_{\text{data}}(\mathbf{Z}|\mathbf{X})) \\ &= \underbrace{\mathbb{E}_{\mathbf{z}_t} \sum_{t=1}^T \log p_{\text{data}}(\mathbf{x}_t|\mathbf{z}_t)}_{-\mathcal{L}_{\text{Recon}}} + \underbrace{\mathbb{E}_{\mathbf{c}} \left[\sum_{t=1}^T \log p_{\text{data}}(\mathbf{z}_t|\mathbf{z}_{\text{HX}}, c_t) - \sum_{t=1}^T \log q_{\phi}(\mathbf{z}_t|\mathbf{x}_t) \right]}_{-\mathcal{L}_{\text{KLD}}} \end{aligned} \quad (14)$$

We use mean-squared error (MSE) for the reconstruction likelihood loss $\mathcal{L}_{\text{Recon}}$. The KL divergence \mathcal{L}_{KLD} is estimated via a sampling approach since with a learned nonparametric transition prior, the distribution does not have an explicit form. Specifically, we obtain the log-likelihood of the posterior, evaluate the prior $\log p(\hat{\mathbf{z}}_t|\hat{\mathbf{z}}_{\text{HX}}, c_t)$ in Eq. (10), and compute their mean difference in the dataset as the KL loss: $\mathcal{L}_{\text{KLD}} = \mathbb{E}_{\hat{\mathbf{z}}_t \sim q(\hat{\mathbf{z}}_t|\mathbf{x}_t)} \log q(\hat{\mathbf{z}}_t|\mathbf{x}_t) - \log p(\hat{\mathbf{z}}_t|\hat{\mathbf{z}}_{\text{HX}}, c_t)$.

5 Experiments

We evaluate the identifiability results of NCTRL on simulated and real-world temporal datasets. We first introduce the evaluation metrics and baselines and then discuss the datasets we used in our experiments. Lastly, we show the experiment results discuss the performance, and make comparisons.

5.1 Evaluation Metrics

Mean Correlation Coefficient (MCC) To evaluate the identifiability of the latent variables, we compute the Mean Correlation Coefficient (MCC) on the test dataset. MCC is a standard metric in the ICA literature for continuous variables which measure the identifiability of the learned latent causal processes. MCC is close to 1.0 when latent variables are identifiable up to permutation and component-wise invertible transformation in the noiseless case.

Mean Square Error (MSE) for estimating \mathbf{A} As introduced in the theory, the \mathbf{A} is identifiable in our setting, which means that our proposed method can provide accurate estimation for the transition matrix \mathbf{A} , to valid such a claim, we use mean square error (MSE) to capture the distance between the estimated $\hat{\mathbf{A}}$ and ground truth \mathbf{A} .

Accuracy for estimating c_t We also test the accuracy for estimating the discrete domain indices c_t supplementary to the MSE for \mathbf{A} since in theory, the \mathbf{A} is identifiable but the c_t is generally not identifiable, which is relatively easy to understand as an analogy in Hidden Markov Models, the transition matrix is identifiable but we can only “infer” the best possible discrete variables but cannot establish identifiability for it.

It is also worth mentioning that the MSE and Accuracy are influenced by the permutation, which is also true in clustering evaluation problems. Here we explored all permutations and selected the best possible assignment for evaluation.

5.2 Baselines

The following identifiable nonlinear ICA methods are used: (1) BetaVAE [23] which ignores both history and nonstationarity information. (2) i-VAE [12] and TCL [9] which leverage nonstationarity to establish identifiability but assume independent factors. (3) SlowVAE [16], and PCL [10] which exploit temporal constraints but assume independent sources and stationary processes. (4) TDRL [18] which assumes nonstationary, causal processes but with observed domain indices. (5) HMNLICA [14] which considers the unobserved nonstationary part in the data generation process but doesn’t allow any causally related time-delayed relations.

5.3 Simulated Results

We generate two synthetic datasets corresponding to different complexity of the nonlinear mixing function g . Both synthetic datasets satisfy our identifiability conditions in the theorems following the procedures in Appendix B.4. As in Table 1, NCTRL can recover the latent processes under unknown nonstationary distribution shifts with high MCCs (>0.95). The baselines that do not exploit history (i.e., BetaVAE, i-VAE, TCL), with independent source assumptions (SlowVAE, PCL), consider limited nonstationary cases (TDRL) distort the identifiability results. The only baseline that considers the unknown nonstationarity in the domain indices (HMNLICA) explored the Markov Assumption but doesn't allow a time-delayed causal process and hence suffers a poor result (MCC 0.58).

On the other hand, the difference between dataset A and dataset B is the nonlinearity in the mixing function, dataset A has a relatively simple nonlinear mixing function, on the contrary, dataset B has more complex nonlinearity. Some variability has been observed among the relative performance ranks of different baselines. For example, i-VAE showed a great discrepancy between the two datasets, which revived the weakness of capturing complex nonlinearity in the unknown nonstationary distribution shift environments. Again we also observed that our proposed method can constantly recover the latent independent components with high MCC

which indicates on both datasets the model is identifiable and the estimation algorithm is highly effective. To further validate if NCTRL successfully recovered the Markov transition matrix \mathbf{A} and

Table 1: Experiment results of two synthetic datasets on baselines and proposed NCTRL, we run the experiments with five different random seeds and calculate the average with standard derivation. The best results are shown in **bold**.

Method	Mean Correlation Coefficien (MCC)		
	Dataset A	Dataset B	Ave.
BetaVAE	44.02 \pm 3.11	47.48 \pm 10.58	45.75
i-VAE	89.74 \pm 3.38	44.50 \pm 0.25	67.12
TCL	37.12 \pm 0.60	56.33 \pm 3.77	46.73
SlowVAE	33.84 \pm 0.60	53.92 \pm 3.56	43.88
PCL	42.41 \pm 2.87	63.66 \pm 2.77	53.04
HMNLICA	59.82 \pm 4.94	57.25 \pm 1.45	58.54
TDRL	83.99 \pm 1.92	72.02 \pm 2.76	78.01
NCTRL	98.85 \pm 0.30	99.01 \pm 0.24	98.93

Table 2: Supplementary experiment results of two synthetic datasets on estimating domain indices c_t and transition matrix \mathbf{A} in NCTRL, we run the experiments with five different random seeds and calculate the average with standard derivation.

Unknown Nonstationary Metrics		
Dataset	Accuracy estimating c_t	MSE estimating \mathbf{A}
A	89.96 \pm 0.24	1.01 $\times 10^{-3}$ \pm 1.67 $\times 10^{-4}$
B	89.84 \pm 0.29	1.08 $\times 10^{-3}$ \pm 1.89 $\times 10^{-4}$

inferred the domain indices c_t with high accuracy. We further examine the accuracy for estimating nonstationary domain indices c_t and the mean square error estimating the transition matrix \mathbf{A} . As shown in Table 2 the result is consistent with our theory in which the transition matrix \mathbf{A} is identifiable and we can estimate it with high accuracy. For the nonstationary domain indices c_t even though there is no identifiability result governing the estimation accuracy, it can still be inferred pretty well since it is nothing but a decoding problem in Hidden Markov Models.

5.4 Real-world Applications

Video data – Modified CartPole Environment We evaluate NCTRL on the modified CartPole [24] video dataset and compare the performances with the baselines. Modified Cartpole is a nonlinear dynamical system with cart positions x_t and pole angles θ_t as the true state variables. The dataset descriptions are in Appendix B.5. Similar to the synthetic dataset, we randomly initialize a Markov chain and roll out a series of c_t , and configure the CartPole environment with respect to the c_t . Specifically, we use five domains with different configurations of cart mass, pole mass, gravity, and noise levels. Together with the two discrete actions (i.e., left and right). By doing so, the nonstationarity is enforced, and since we can control and access all intermediate states in the system, all metrics including MCC and c_t accuracy together with \mathbf{A} MSE can be easily calculated. We fit

NCTRL with two-dimensional causal factors. We set the latent size $n = 2$ and the lag number $L = 2$. In Fig. 4, the latent causal processes are recovered, as seen from (a) high MCC for the latent causal processes; (b) the latent factors are estimated up to component-wise transformation; and (c) the latent traversals confirm the two recovered latent variables correspond to the position and pole angle.

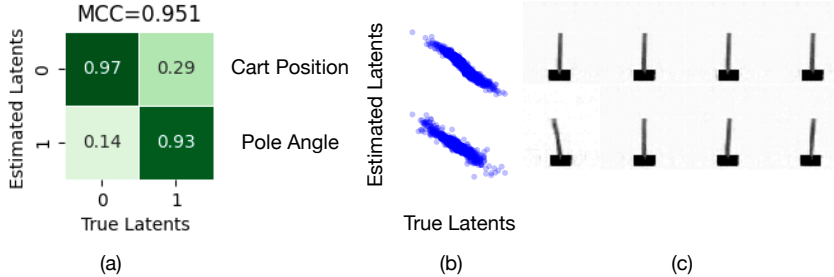


Figure 4: Modified Cartpole results: (a) MCC for causally-related factors; (b) scatterplots between estimated and true factors; and (c) latent traversal on a fixed video frame

Table 3: Experiment results of CartPole dataset. The best results are shown in **bold**.

Mean Correlation Coefficient (MCC)						
BetaVAE	i-VAE	TCL	SlowVAE	SKD	TDRL	NCTRL
57.54	60.14	65.07	63.16	73.24	85.26	96.06

Table 4: Supplementary experiment results of CartPole datasets on estimating domain indices c_t and transition matrix \mathbf{A} in NCTRL, we run the experiments with five different random seeds and calculate the average with standard derivation.

Unknown Nonstationary Metrics	
Accuracy estimating c_t	MSE estimating \mathbf{A}
79.23 ± 5.33	$5.01 \times 10^{-2} \pm 1.23 \times 10^{-2}$

Similar to Table 1 and 2, we compare our NCTRL with baseline methods. In addition, we also compare with SKD [25], a state-of-the-art sequential disentangle representation learning method without identifiability guarantee. In Table 3 and 4 we can see that compared with TDRL, our NCTRL can recover the latent processes under unknown nonstationary distribution shifts with high MCCs (>0.95) with highly accurate estimated transition matrix \mathbf{A} and high quality inferred c_t . Specifically, by comparing the result of SKD, the MCC for SKD is better than a variety of baselines, however, we can see the distinction between well-disentangled models and identifiable models, only the models with identifiability can find the ground truth latent variables with theoretical guarantee.

Video data – MoSeq Dataset We test NCTRL framework to analyze mouse behavior video data from Wiltchko et al. [19], which represents the original application to clustering mouse behavior⁴, details of this dataset are available in Appendix B.6. Since there are no ground truth independent components in this particular real-world dataset, we analyze it by several visualizations to see if different domains can be properly identified and if the patterns in the recovered independent components are consistent with the recovered domain indices. We analyze the first video clip of mouse behavior data and visualize the two phases we discovered and segmented in Fig 5. We can clearly see from Fig 5 that there are different phases with the upper one actively moving and the lower one inactive. The recovered independent components showed a consistent pattern with the recovered phase or domain indices as shown in Fig 5.

⁴Dataset can be accessed via <https://dattalab.github.io/moseq2-website/index.html>

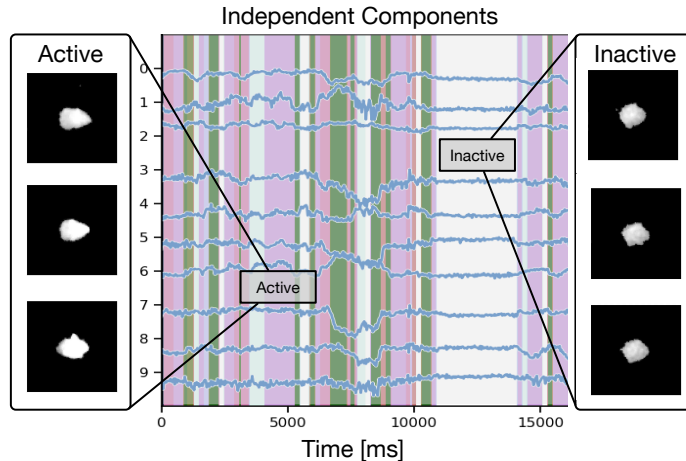


Figure 5: Result visualization of MoSeq dataset. (Active, Inactive) show two representative video frames for the active and inactive phases and (Independent Components) visualize the discovered independent components with corresponding phases tagged with different colors.

6 Related Work

Causal Discovery from Time Series Understanding the causal structure in time-series data is pivotal in areas such as machine learning [1], econometrics [2], and neuroscience [3]. A bulk of the research in this realm emphasizes determining the temporal causal links among observed variables. The primary techniques employed are constraint-based methods [26], which use conditional independence tests to ascertain causal structures, and score-based methods [27, 28], where scores are utilized to oversee a search operation. Some researchers also proposed a combination of these two methods [29, 30]. Additionally, Granger causality [31] and its nonlinear adaptations [32, 33] have gained widespread acceptance in this context.

Nonlinear ICA for Time Series Recently, the significance of temporal structures and non-stationarities has been recognized in achieving identifiability within nonlinear ICA. Time-contrastive learning (TCL [9]) utilizes the independent sources principle, focusing on data segments’ variability. On the other hand, Permutation-based contrastive (PCL [10]) offers a learning approach that distinguishes true independent sources from shuffled ones under the uniformly dependent assumption. HMNLICA [14] integrates nonlinear ICA with an HMM to address non-stationarity without segmenting data manually. The i-VAE [12] approach employs VAEs to capture the actual joint distribution between observed and auxiliary non-stationary domains, assuming an exponential families conditional distribution. The recent advancements in nonlinear ICA for time series include LEAP [17], (i-)CITRIS [34, 35], and TDRL [18]. While LEAP introduces a novel condition emphasizing non-stationary noise, TDRL delves deeper into a non-parametric environment within a nonstationary context. In contrast, CITRIS recommends utilizing intervention target data for pinpointing latent causal aspects, avoiding certain constraints but necessitating active intervention access.

Sequential Disentanglement Majority of existing work about sequential disentanglement focuses on architecture based on dynamical variational autoencoder (VAE) [36]. Early works [37, 38] separate dynamic factors from static factors using probabilistic methods. Then auxiliary tasks with self-supervisory signals [39] were introduced. C-DSVAE [40] utilized contrastive penalty terms with data augmentation to introduce additional inductive biases. In R-WAE [41], Wasserstein distance was introduced to replace KL divergence. To deal with video disentanglement [42, 43] explored generative adversarial network (GAN) architectures and [44] introduced a recurrent model with adversarial loss. FAVAE, [45] proposed a factorizing VAE and [46] proposed to learn hierarchical features. Finally, SKD [25] introduced a spectral loss term that leads to structured Koopman matrices and disentanglement.

7 Conclusion and Discussion

Conclusion. In this paper, we first established an identifiability theory for general sequential data with nonstationary causally-related processes under unknown distribution shifts. Then we presented NCTRL, a principled framework to recover the time-delayed latent causal variable identify their causal relations from measured data, and decode high-quality domain indices under Markov assumption. Experiment results on both synthetic datasets and real-world video datasets showed that our proposed method can recover the latent causal variables and their causal relations purely from measured data with the observation of auxiliary variables or domain indices.

Limitation. The basic limitation of this work is that the nonstationary domain indices are assumed to follow a Markov chain. Also, this work highly relies on the latent processes to have no instantaneous causal relations but only time-delayed influences. If the resolution of the time series is much lower, then it is usually violated and one has to find a way to deal with instantaneous causal relations. Extending our theories and framework to address the scenarios when more flexibility in the domain indices transition is allowed (i.e. beyond discrete variables following a Markov chain) and to address instantaneous dependency or instantaneous causal relations will be some of our future work.

Boarder Impacts. This work proposes a theoretical analysis and technical methods to learn the causal representation from time-series data, which facilitate the construction of more transparent and interpretable models to understand the causal effect in the real world. This could be beneficial in a variety of sectors, including healthcare, finance, and technology. In contrast, misinterpretations of causal relationships could also have significant negative implications in these fields, which must be carefully done to avoid unfair or biased predictions.

8 Acknowledgment

This project has been graciously funded by NGA HM04762010002, NSF IIS1955532, NSF CNS2008248, NIGMS R01GM140467, NSF IIS2123952, NSF BCS2040381, an Amazon Research Award, NSF IIS2311990, and DARPA ECOLE HR00112390063. This project is also partially supported by NSF Grant 2229881, the National Institutes of Health (NIH) under Contract R01HL159805, a grant from Apple Inc., a grant from KDDI Research Inc., and generous gifts from Salesforce Inc., Microsoft Research, and Amazon Research. We also extend our sincere thanks to Yingzhen Li and Carles Balsells-Rodas for the insightful discussion on the identifiability result in this paper.

References

- [1] Carlo Berzuini, Philip Dawid, and Luisa Bernardinell. *Causality: Statistical perspectives and applications*. John Wiley & Sons, 2012.
- [2] Eric Ghysels, Jonathan B Hill, and Kaiji Motegi. Testing for granger causality with mixed frequency data. *Journal of Econometrics*, 192(1):207–230, 2016.
- [3] Karl Friston. Causal modelling and brain connectivity in functional magnetic resonance imaging. *PLoS biology*, 7(2):e1000033, 2009.
- [4] Clive WJ Granger. Testing for causality: A personal viewpoint. *Journal of Economic Dynamics and control*, 2:329–352, 1980.
- [5] Mingming Gong, Kun Zhang, Bernhard Schölkopf, Dacheng Tao, and Philipp Geiger. Discovering temporal causal relations from subsampled data. In *International Conference on Machine Learning*, pages 1898–1906. PMLR, 2015.
- [6] Aapo Hyvärinen, Kun Zhang, Shohei Shimizu, and Patrik O Hoyer. Estimation of a structural vector autoregression model using non-gaussianity. *Journal of Machine Learning Research*, 11(5), 2010.
- [7] Francesco Locatello, Stefan Bauer, Mario Lucic, Gunnar Raetsch, Sylvain Gelly, Bernhard Schölkopf, and Olivier Bachem. Challenging common assumptions in the unsupervised learning of disentangled representations. In *international conference on machine learning*, pages 4114–4124. PMLR, 2019.

- [8] Aapo Hyvärinen and Petteri Pajunen. Nonlinear independent component analysis: Existence and uniqueness results. *Neural networks*, 12(3):429–439, 1999.
- [9] Aapo Hyvärinen and Hiroshi Morioka. Unsupervised feature extraction by time-contrastive learning and nonlinear ica. *Advances in Neural Information Processing Systems*, 29:3765–3773, 2016.
- [10] Aapo Hyvärinen and Hiroshi Morioka. Nonlinear ica of temporally dependent stationary sources. In *Artificial Intelligence and Statistics*, pages 460–469. PMLR, 2017.
- [11] Aapo Hyvärinen, Hiroaki Sasaki, and Richard Turner. Nonlinear ica using auxiliary variables and generalized contrastive learning. In *The 22nd International Conference on Artificial Intelligence and Statistics*, pages 859–868. PMLR, 2019.
- [12] Ilyes Khemakhem, Diederik Kingma, Ricardo Monti, and Aapo Hyvärinen. Variational autoencoders and nonlinear ica: A unifying framework. In *International Conference on Artificial Intelligence and Statistics*, pages 2207–2217. PMLR, 2020.
- [13] Peter Sorrenson, Carsten Rother, and Ullrich Köthe. Disentanglement by nonlinear ica with general incompressible-flow networks (gin). *arXiv preprint arXiv:2001.04872*, 2020.
- [14] Hermanni Hälvä and Aapo Hyvärinen. Hidden markov nonlinear ica: Unsupervised learning from nonstationary time series. In *Conference on Uncertainty in Artificial Intelligence*, pages 939–948. PMLR, 2020.
- [15] Hermanni Hälvä, Sylvain Le Corff, Luc Lehéricy, Jonathan So, Yongjie Zhu, Elisabeth Gassiat, and Aapo Hyvärinen. Disentangling identifiable features from noisy data with structured nonlinear ica. *arXiv preprint arXiv:2106.09620*, 2021.
- [16] David Klindt, Lukas Schott, Yash Sharma, Ivan Ustyuzhaninov, Wieland Brendel, Matthias Bethge, and Dylan Paiton. Towards nonlinear disentanglement in natural data with temporal sparse coding. *arXiv preprint arXiv:2007.10930*, 2020.
- [17] Weiran Yao, Yuewen Sun, Alex Ho, Changyin Sun, and Kun Zhang. Learning temporally causal latent processes from general temporal data. In *International Conference on Learning Representations*, 2022. URL <https://openreview.net/forum?id=RD1LMjLJXdq>.
- [18] Weiran Yao, Guangyi Chen, and Kun Zhang. Temporally disentangled representation learning. In Alice H. Oh, Alekh Agarwal, Danielle Belgrave, and Kyunghyun Cho, editors, *Advances in Neural Information Processing Systems*, 2022. URL https://openreview.net/forum?id=Vi-sZWNA_Ue.
- [19] Alexander B. Wiltschko, Matthew J. Johnson, Giuliano Iurilli, Ralph E. Peterson, Jesse M. Katon, Stan L. Pashkovski, Victoria E. Abaira, Ryan P. Adams, and Sandeep Robert Datta. Mapping sub-second structure in mouse behavior. *Neuron*, 88(6):1121–1135, 2015. ISSN 0896-6273. doi: <https://doi.org/10.1016/j.neuron.2015.11.031>. URL <https://www.sciencedirect.com/science/article/pii/S0896627315010375>.
- [20] Élisabeth Gassiat, Alice Cleynen, and Stephane Robin. Inference in finite state space non parametric hidden markov models and applications. *Statistics and Computing*, 26:61–71, 2016.
- [21] Carles Balsells-Rodas, Yixin Wang, and Yingzhen Li. On the identifiability of markov switching models. In *ICML 2023 Workshop on Structured Probabilistic Inference & Generative Modeling*, 2023. URL <https://openreview.net/forum?id=lnPoe39GEs>.
- [22] Li Yingzhen and Stephan Mandt. Disentangled sequential autoencoder. In *International Conference on Machine Learning*, pages 5670–5679. PMLR, 2018.
- [23] Irina Higgins, Loic Matthey, Arka Pal, Christopher Burgess, Xavier Glorot, Matthew Botvinick, Shakir Mohamed, and Alexander Lerchner. beta-VAE: Learning basic visual concepts with a constrained variational framework. In *International Conference on Learning Representations*, 2017. URL <https://openreview.net/forum?id=Sy2fzU9g1>.

- [24] Biwei Huang, Fan Feng, Chaochao Lu, Sara Magliacane, and Kun Zhang. Adarl: What, where, and how to adapt in transfer reinforcement learning. *arXiv preprint arXiv:2107.02729*, 2021.
- [25] Nimrod Berman, Ilan Naiman, and Omri Azencot. Multifactor sequential disentanglement via structured koopman autoencoders. In *The Eleventh International Conference on Learning Representations*, 2023. URL <https://openreview.net/forum?id=6fuPIe9tbnC>.
- [26] Doris Entner and Patrik O Hoyer. On causal discovery from time series data using fci. *Probabilistic graphical models*, pages 121–128, 2010.
- [27] Kevin P Murphy et al. Dynamic bayesian networks. *Probabilistic Graphical Models*, M. Jordan, 7:431, 2002.
- [28] Roxana Pamfil, Nisara Sriwattanaworachai, Shaan Desai, Philip Pilgerstorfer, Konstantinos Georgatzis, Paul Beaumont, and Bryon Aragam. Dynotears: Structure learning from time-series data. In *International Conference on Artificial Intelligence and Statistics*, pages 1595–1605. PMLR, 2020.
- [29] Daniel Malinsky and Peter Spirtes. Causal structure learning from multivariate time series in settings with unmeasured confounding. In *Proceedings of 2018 ACM SIGKDD Workshop on Causal Discovery*, pages 23–47. PMLR, 2018.
- [30] Daniel Malinsky and Peter Spirtes. Learning the structure of a nonstationary vector autoregression. In *The 22nd International Conference on Artificial Intelligence and Statistics*, pages 2986–2994. PMLR, 2019.
- [31] Clive WJ Granger. Investigating causal relations by econometric models and cross-spectral methods. *Econometrica: journal of the Econometric Society*, pages 424–438, 1969.
- [32] Alex Tank, Ian Covert, Nicholas Foti, Ali Shojaie, and Emily Fox. Neural granger causality. *arXiv preprint arXiv:1802.05842*, 2018.
- [33] Sindy Löwe, David Madras, Richard Zemel, and Max Welling. Amortized causal discovery: Learning to infer causal graphs from time-series data. *arXiv preprint arXiv:2006.10833*, 2020.
- [34] Phillip Lippe, Sara Magliacane, Sindy Löwe, Yuki M Asano, Taco Cohen, and Stratis Gavves. Citris: Causal identifiability from temporal intervened sequences. In *International Conference on Machine Learning*, pages 13557–13603. PMLR, 2022.
- [35] Phillip Lippe, Sara Magliacane, Sindy Löwe, Yuki M Asano, Taco Cohen, and Efstratios Gavves. icitris: Causal representation learning for instantaneous temporal effects. *arXiv preprint arXiv:2206.06169*, 2022.
- [36] Laurent Girin, Simon Leglaive, Xiaoyu Bie, Julien Diard, Thomas Hueber, and Xavier Alameda-Pineda. *Dynamical Variational Autoencoders: A Comprehensive Review*. 2021.
- [37] Wei-Ning Hsu, Yu Zhang, and James Glass. Unsupervised learning of disentangled and interpretable representations from sequential data. *Advances in neural information processing systems*, 30, 2017.
- [38] Yingzhen Li and Stephan Mandt. Disentangled sequential autoencoder. *arXiv preprint arXiv:1803.02991*, 2018.
- [39] Yizhe Zhu, Martin Renqiang Min, Asim Kadav, and Hans Peter Graf. S3VAE: Self-supervised sequential VAE for representation disentanglement and data generation. In *Proceedings of the IEEE/CVF Conference on Computer Vision and Pattern Recognition*, pages 6538–6547, 2020.
- [40] Junwen Bai, Weiran Wang, and Carla P Gomes. Contrastively disentangled sequential variational autoencoder. *Advances in Neural Information Processing Systems*, 34, 2021.
- [41] Jun Han, Martin Renqiang Min, Ligong Han, Li Erran Li, and Xuan Zhang. Disentangled recurrent wasserstein autoencoder. In *International Conference on Learning Representations*, 2021. URL <https://openreview.net/forum?id=07ms4LFdsX>.

- [42] Ruben Villegas, Jimei Yang, Seunghoon Hong, Xunyu Lin, and Honglak Lee. Decomposing motion and content for natural video sequence prediction. In *International Conference on Learning Representations*, 2017. URL <https://openreview.net/forum?id=rkEFLFqee>.
- [43] Sergey Tulyakov, Ming-Yu Liu, Xiaodong Yang, and Jan Kautz. Mocogan: Decomposing motion and content for video generation. In *Proceedings of the IEEE conference on computer vision and pattern recognition*, pages 1526–1535, 2018.
- [44] Emily L Denton and Vishnesh Birodkar. Unsupervised learning of disentangled representations from video. *Advances in neural information processing systems*, 30, 2017.
- [45] Masanori Yamada, Heecheol Kim, Kosuke Miyoshi, Tomoharu Iwata, and Hiroshi Yamakawa. Disentangled representations for sequence data using information bottleneck principle. In *Asian Conference on Machine Learning*, pages 305–320. PMLR, 2020.
- [46] Shengjia Zhao, Jiaming Song, and Stefano Ermon. Learning hierarchical features from deep generative models. In Doina Precup and Yee Whye Teh, editors, *Proceedings of the 34th International Conference on Machine Learning*, volume 70 of *Proceedings of Machine Learning Research*, pages 4091–4099. PMLR, 06–11 Aug 2017. URL <https://proceedings.mlr.press/v70/zhao17c.html>.
- [47] Guillaume Morel, Lucas Drumetz, Simon Benaïchouche, Nicolas Courty, and François Rousseau. Turning normalizing flows into monge maps with geodesic gaussian preserving flows. *Transactions on Machine Learning Research*, 2023. ISSN 2835-8856. URL <https://openreview.net/forum?id=2UQv8L1Cv9>.
- [48] Alessio Spantini, Daniele Bigoni, and Youssef Marzouk. Inference via low-dimensional couplings. *The Journal of Machine Learning Research*, 19(1):2639–2709, 2018.

Supplement to

“Temporally Disentangled Representation Learning under Unknown Nonstationarity”

Appendix organization:

A	Identifiability	16
A.1	Identifiability of Nonstationary Hidden States	16
A.2	Identifiability of Latent Causal Processes	17
A.3	Discussion on Assumptions in Theorem 2	18
B	Implementation Details	19
B.1	Reproducibility	19
B.2	Prior Likelihood Derivation	19
B.3	Derivation of ELBO	20
B.4	Synthetic Dataset Generation	21
B.4.1	Sample c_t from Markov chain	21
B.4.2	Generation of latent variables \mathbf{z}_t	21
B.4.3	Generation of observations \mathbf{x}_t	21
B.5	Modified CartPole Dataset Generation	21
B.6	MoSeq Dataset	21
B.7	Mean Correlation Coefficient	21
B.8	Network Architecture	22
C	Note on updated proof for identifiability of the nonstationary part	22

A Identifiability

Assume we observe n -dimensional time-series data at discrete time steps, $\mathbf{X} = \{\mathbf{x}_1, \mathbf{x}_2, \dots, \mathbf{x}_T\}$, where each \mathbf{x}_t is generated from time-delayed causally related hidden components $\mathbf{z}_t \in \mathbb{R}^n$ by the invertible mixing function:

$$\mathbf{x}_t = \mathbf{g}(\mathbf{z}_t). \quad (1)$$

In addition to latent components \mathbf{z}_t , there is an extra hidden component c_t which is a discrete variable with cardinality $|c_t| = C$, it follows first-order Markov process controlled by a $C \times C$ transition matrix \mathbf{A} , in which the i, j -th entry $A_{i,j}$ is the probability to transit from state i to j .

$$c_1, c_2, \dots, c_t \sim \text{Markov Chain}(\mathbf{A}) \quad (2)$$

For $i \in \{1, \dots, n\}$, z_{it} , as the i -th component of \mathbf{z}_t , is generated by (some) components of history information \mathbf{z}_{t-1} , discrete nonstationary indicator c_t , and noise ϵ_{it} .

$$z_{it} = f_i(\{z_{j,t-1} \mid z_{j,t-\tau} \in \mathbf{Pa}(z_{it})\}, c_t, \epsilon_{it}) \quad \text{with} \quad \epsilon_{it} \sim p_{\epsilon_i | c_t} \quad (3)$$

where $\mathbf{Pa}(z_{it})$ is the set of latent factors that directly cause z_{it} , which can be any subset of $\mathbf{z}_{\text{HX}} = \{\mathbf{z}_{t-1}, \mathbf{z}_{t-2}, \dots, \mathbf{z}_{t-L}\}$ up to history information maximum lag L . The components of \mathbf{z}_t are mutually independent conditional on \mathbf{z}_{HX} and c_t .

A.1 Identifiability of Nonstationary Hidden States

Theorem A.1 (identifiability of nonstationary hidden states). *Suppose the observed data is generated following the nonlinear ICA framework as defined in Eqs. (1), (2) and (3). And suppose the following assumptions hold:*

- i The transition in Eq. (3) is in Gaussian family, and the transition functions f_i are analytic.*
- ii The mixing function in Eq. (1) together with its inverse are analytic and preserve volume in terms of Def. 3.*

Then the Markov switching model is identifiable in terms of Def. 2.

Proof. Since the transition in Eq. (3) is in Gaussian family, the conditional density function $p(\mathbf{z}_t \mid \mathbf{z}_{t-1}, c_t)$ can be expressed as

$$p(\mathbf{z}_t \mid \mathbf{z}_{t-1}, c_t) = \mathcal{N}(\mathbf{m}(\mathbf{z}_{t-1}, c_t), \mathbf{\Sigma}(\mathbf{z}_{t-1}, c_t)) \quad (4)$$

which is Gaussian family and since for different value of c_t the transition functions are not identical then the unique indexing is also satisfied.

Then the latent \mathbf{z}_t are passed through the mixing function which is invertible and volume-preserving. Considering such mapping \mathbf{g} from \mathbf{z}_t to \mathbf{x}_t :

$$p(\mathbf{z}_t \mid \mathbf{z}_{t-1}, c_t) = p(\mathbf{z}_t \mid \mathbf{x}_{t-1}, c_t) = p(\mathbf{x}_t \mid \mathbf{x}_{t-1}, c_t) \cdot |\mathbf{J}_{\mathbf{g}}| \quad (5)$$

Since \mathbf{g} is volume-preserving, $|\mathbf{J}_{\mathbf{g}}| = 1$, $p(\mathbf{z}_t \mid \mathbf{z}_{t-1}, c_t)$ is gaussian implies $p(\mathbf{x}_t \mid \mathbf{x}_{t-1}, c_t)$ is also gaussian. The unique indexing of $p(\mathbf{z}_t \mid \mathbf{z}_{t-1}, c_t)$ together with the invertibility of \mathbf{g} implies the unique indexing of $p(\mathbf{x}_t \mid \mathbf{x}_{t-1}, c_t)$. Similar arguments can be made for initial distributions.

Lastly, we can construct an analytic function for the mean, $\mathbf{m}(\mathbf{x}_{t-1}, c_t) = \mathbf{g} \circ \mathbf{f}(\mathbf{g}^{-1}(\mathbf{x}_{t-1}), c_t)$. Similar construction can be made for variance, even though it may be hard to write down the explicit form, it still is analytic.

Then the conclusion of Lemma 1 applies, which gives the identifiability of the Markov switching part up to permutation as defined in Def. 2. \square

Note that the analytic form requirement is to ensure that the intersection of moments has zero measure from unique indexing. In our case, this property comes purely from the unique indexing for the mean, which does not actually require the analytical form for the variance. In addition, volume-preserving constraints can be further relaxed for any Gaussian-preserving transformation that is discussed in [47]. Furthermore, the Gaussian family assumption here may also be relaxed as long as the linear independence property described in [21] can be fulfilled, and correspondingly, the Gaussian preserving transformation can also be further relaxed. We leave those discussions in future work.

A.2 Identifiability of Latent Causal Processes

To incorporate nonlinear ICA into the Markov Assumption we define the emission distribution $p(\mathbf{x}_t | \mathbf{x}_{t-1}, c_t)$ as a deep latent variable model. First, the latent independent component variables $\mathbf{z}_t \in \mathbb{R}^n$ are generated from a factorial prior, given the hidden state c_t and previous \mathbf{z}_{t-1} , as

$$p(\mathbf{z}_t | \mathbf{z}_{t-1}, c_t) = \prod_{k=1}^n p(z_{kt} | \mathbf{z}_{t-1}, c_t). \quad (6)$$

Second, the observed data $\mathbf{x}_t \in \mathbb{R}^n$ is generated by a nonlinear mixing function as in Eq. (1) which is assumed to be bijective with inverse given by $\mathbf{z}_t = \mathbf{g}^{-1}(\mathbf{x}_t)$. Let $\eta_{kt}(c_t) \triangleq \log p(z_{kt} | \mathbf{z}_{t-1}, c_t)$, and assume that $\eta_{kt}(c_t)$ is twice differentiable in z_{kt} and is differentiable in $z_{l,t-1}$, $l = 1, 2, \dots, n$. Note that the parents of z_{kt} may be only c_t and a subset of \mathbf{z}_{t-1} ; if $z_{l,t-1}$ is not a parent of z_{kt} , then $\frac{\partial \eta_{kt}}{\partial z_{l,t-1}} = 0$.

Theorem A.2. *Suppose there exists an invertible function $\hat{\mathbf{g}}^{-1}$, which is the estimated demixing function that maps \mathbf{x}_t to $\hat{\mathbf{z}}_t$, i.e.,*

$$\hat{\mathbf{z}}_t = \hat{\mathbf{g}}^{-1}(\mathbf{x}_t) \quad (7)$$

such that the components of $\hat{\mathbf{z}}_t$ are mutually independent conditional on $\hat{\mathbf{z}}_{t-1}$. Let

$$\begin{aligned} \mathbf{v}_{k,t}(c) &\triangleq \left(\frac{\partial^2 \eta_{kt}(c)}{\partial z_{k,t} \partial z_{1,t-1}}, \frac{\partial^2 \eta_{kt}(c)}{\partial z_{k,t} \partial z_{2,t-1}}, \dots, \frac{\partial^2 \eta_{kt}(c)}{\partial z_{k,t} \partial z_{n,t-1}} \right)^\top, \\ \hat{\mathbf{v}}_{k,t}(c) &\triangleq \left(\frac{\partial^3 \eta_{kt}(c)}{\partial z_{k,t}^2 \partial z_{1,t-1}}, \frac{\partial^3 \eta_{kt}(c)}{\partial z_{k,t}^2 \partial z_{2,t-1}}, \dots, \frac{\partial^3 \eta_{kt}(c)}{\partial z_{k,t}^2 \partial z_{n,t-1}} \right)^\top. \end{aligned} \quad (8)$$

And

$$\begin{aligned} \mathbf{s}_{kt} &\triangleq \left(\mathbf{v}_{kt}(1)^\top, \dots, \mathbf{v}_{kt}(C)^\top, \frac{\partial^2 \eta_{kt}(2)}{\partial z_{kt}^2} - \frac{\partial^2 \eta_{kt}(1)}{\partial z_{kt}^2}, \dots, \frac{\partial^2 \eta_{kt}(C)}{\partial z_{kt}^2} - \frac{\partial^2 \eta_{kt}(C-1)}{\partial z_{kt}^2} \right)^\top, \\ \hat{\mathbf{s}}_{kt} &\triangleq \left(\hat{\mathbf{v}}_{kt}(1)^\top, \dots, \hat{\mathbf{v}}_{kt}(C)^\top, \frac{\partial \eta_{kt}(2)}{\partial z_{kt}} - \frac{\partial \eta_{kt}(1)}{\partial z_{kt}}, \dots, \frac{\partial \eta_{kt}(C)}{\partial z_{kt}} - \frac{\partial \eta_{kt}(C-1)}{\partial z_{kt}} \right)^\top. \end{aligned} \quad (9)$$

If for each value of \mathbf{z}_t , $\mathbf{s}_{1t}, \hat{\mathbf{s}}_{1t}, \mathbf{v}_{2t}, \hat{\mathbf{s}}_{2t}, \dots, \mathbf{s}_{nt}, \hat{\mathbf{s}}_{nt}$, as $2n$ function vectors $\mathbf{s}_{k,t}$ and $\hat{\mathbf{s}}_{k,t}$, with $k = 1, 2, \dots, n$, are linearly independent, then $\hat{\mathbf{z}}_t$ must be an invertible, component-wise transformation of a permuted version of \mathbf{z}_t .

Proof. Combining (1) and (7) gives $\mathbf{z}_t = (\mathbf{g}^{-1} \circ \hat{\mathbf{g}})(\hat{\mathbf{z}}_t) = \mathbf{h}(\hat{\mathbf{z}}_t)$, where $\mathbf{h} \triangleq \mathbf{g}^{-1} \circ \hat{\mathbf{g}}$. Since both \mathbf{g} and $\hat{\mathbf{g}}$ are invertible, \mathbf{h} is invertible. Let \mathbf{H}_t be the Jacobian matrix of the transformation $\mathbf{h}(\hat{\mathbf{z}}_t)$, and denote by \mathbf{H}_{kit} its (k, i) th entry.

First, it is straightforward to see that if the components of $\hat{\mathbf{z}}_t$ are mutually independent conditional on previous $\hat{\mathbf{z}}_{t-1}$ and current c_t , then for any $i \neq j$, \hat{z}_{it} and \hat{z}_{jt} are conditionally independent given $\hat{\mathbf{z}}_{t-1} \cup (\hat{\mathbf{z}}_t \setminus \{\hat{z}_{it}, \hat{z}_{jt}\}) \cup \{c_t\}$. Mutual independence of the components of $\hat{\mathbf{z}}_t$ conditional on $\hat{\mathbf{z}}_{t-1}$ implies that \hat{z}_{it} is independent from $\hat{\mathbf{z}}_t \setminus \{\hat{z}_{it}, \hat{z}_{jt}\}$ conditional on $\hat{\mathbf{z}}_{t-1}$ and c_t , i.e.,

$$p(\hat{z}_{it} | \hat{\mathbf{z}}_{t-1}, c_t) = p(\hat{z}_{it} | \hat{\mathbf{z}}_{t-1} \cup (\hat{\mathbf{z}}_t \setminus \{\hat{z}_{it}, \hat{z}_{jt}\}), c_t).$$

At the same time, it also implies \hat{z}_{it} is independent from $\hat{\mathbf{z}}_t \setminus \{\hat{z}_{it}\}$ conditional on $\hat{\mathbf{z}}_{t-1}$ and c_t , i.e.,

$$p(\hat{z}_{it} | \hat{\mathbf{z}}_{t-1}, c_t) = p(\hat{z}_{it} | \hat{\mathbf{z}}_{t-1} \cup (\hat{\mathbf{z}}_t \setminus \{\hat{z}_{it}\}), c_t).$$

Combining the above two equations gives

$$p(\hat{z}_{it} | \hat{\mathbf{z}}_{t-1} \cup (\hat{\mathbf{z}}_t \setminus \{\hat{z}_{it}\}), c_t) = p(\hat{z}_{it} | \hat{\mathbf{z}}_{t-1} \cup (\hat{\mathbf{z}}_t \setminus \{\hat{z}_{it}, \hat{z}_{jt}\}), c_t),$$

i.e., for $i \neq j$, \hat{z}_{it} and \hat{z}_{jt} are conditionally independent given $\hat{\mathbf{z}}_{t-1} \cup (\hat{\mathbf{z}}_t \setminus \{\hat{z}_{it}, \hat{z}_{jt}\}) \cup \{c_t\}$.

We then make use of the fact that if \hat{z}_{it} and \hat{z}_{jt} are conditionally independent given $\hat{\mathbf{z}}_{t-1} \cup (\hat{\mathbf{z}}_t \setminus \{\hat{z}_{it}, \hat{z}_{jt}\}) \cup \{c_t\}$, then

$$\frac{\partial^2 \log p(\hat{\mathbf{z}}_t, \hat{\mathbf{z}}_{t-1}, c_t)}{\partial \hat{z}_{it} \partial \hat{z}_{jt}} = 0,$$

assuming the cross second-order derivative exists [48]. Since $p(\hat{\mathbf{z}}_t, \hat{\mathbf{z}}_{t-1}, c_t) = p(\hat{\mathbf{z}}_t | \hat{\mathbf{z}}_{t-1}, c_t)p(\hat{\mathbf{z}}_{t-1}, c_t)$ while $p(\hat{\mathbf{z}}_{t-1}, c_t)$ does not involve \hat{z}_{it} or \hat{z}_{jt} , the above equality is equivalent to

$$\frac{\partial^2 \log p(\hat{\mathbf{z}}_t | \hat{\mathbf{z}}_{t-1}, c_t)}{\partial \hat{z}_{it} \partial \hat{z}_{jt}} = 0. \quad (10)$$

Then for any c_t , the Jacobian matrix of the mapping from $(\mathbf{x}_{t-1}, \hat{\mathbf{z}}_t)$ to $(\mathbf{x}_{t-1}, \mathbf{z}_t)$ is $\begin{bmatrix} \mathbf{I} & \mathbf{0} \\ * & \mathbf{H}_t \end{bmatrix}$, where $*$ stands for a matrix, and the (absolute value of the) determinant of this Jacobian matrix is $|\mathbf{H}_t|$. Therefore $p(\hat{\mathbf{z}}_t, \mathbf{x}_{t-1} | c_t) = p(\mathbf{z}_t, \mathbf{x}_{t-1} | c_t) \cdot |\mathbf{H}_t|$. Dividing both sides of this equation by $p(\mathbf{x}_{t-1} | c_t)$ gives

$$p(\hat{\mathbf{z}}_t | \mathbf{x}_{t-1}, c_t) = p(\mathbf{z}_t | \mathbf{x}_{t-1}, c_t) \cdot |\mathbf{H}_t|. \quad (11)$$

Since $p(\mathbf{z}_t | \mathbf{z}_{t-1}, c_t) = p(\mathbf{z}_t | \mathbf{g}(\mathbf{z}_{t-1}), c_t) = p(\mathbf{z}_t | \mathbf{x}_{t-1}, c_t)$ and similarly $p(\hat{\mathbf{z}}_t | \hat{\mathbf{z}}_{t-1}, c_t) = p(\hat{\mathbf{z}}_t | \mathbf{x}_{t-1}, c_t)$, Eq. 11 tells us

$$\log p(\hat{\mathbf{z}}_t | \hat{\mathbf{z}}_{t-1}, c_t) = \log p(\mathbf{z}_t | \mathbf{z}_{t-1}, c_t) + \log |\mathbf{H}_t| = \sum_{k=1}^n \eta_{kt}(c_t) + \log |\mathbf{H}_t|. \quad (12)$$

Its partial derivative w.r.t. \hat{z}_{it} is

$$\begin{aligned} \frac{\partial \log p(\hat{\mathbf{z}}_t | \hat{\mathbf{z}}_{t-1}, c_t)}{\partial \hat{z}_{it}} &= \sum_{k=1}^n \frac{\partial \eta_{kt}(c_t)}{\partial z_{kt}} \cdot \frac{\partial z_{kt}}{\partial \hat{z}_{it}} - \frac{\partial \log |\mathbf{H}_t|}{\partial \hat{z}_{it}} \\ &= \sum_{k=1}^n \frac{\partial \eta_{kt}(c_t)}{\partial z_{kt}} \cdot \mathbf{H}_{kit} - \frac{\partial \log |\mathbf{H}_t|}{\partial \hat{z}_{it}}. \end{aligned}$$

Its second-order cross-derivative is

$$\frac{\partial^2 \log p(\hat{\mathbf{z}}_t | \hat{\mathbf{z}}_{t-1}, c_t)}{\partial \hat{z}_{it} \partial \hat{z}_{jt}} = \sum_{k=1}^n \left(\frac{\partial^2 \eta_{kt}(c_t)}{\partial z_{kt}^2} \cdot \mathbf{H}_{kit} \mathbf{H}_{kjt} + \frac{\partial \eta_{kt}(c_t)}{\partial z_{kt}} \cdot \frac{\partial \mathbf{H}_{kit}}{\partial \hat{z}_{jt}} \right) - \frac{\partial^2 \log |\mathbf{H}_t|}{\partial \hat{z}_{it} \partial \hat{z}_{jt}}. \quad (13)$$

The above quantity is always 0 according to Eq. (10). Therefore, for each $l = 1, 2, \dots, n$ and each value $z_{l,t-1}$, its partial derivative w.r.t. $z_{l,t-1}$ is always 0. That is,

$$\frac{\partial^3 \log p(\hat{\mathbf{z}}_t | \hat{\mathbf{z}}_{t-1}, c_t)}{\partial \hat{z}_{it} \partial \hat{z}_{jt} \partial z_{l,t-1}} = \sum_{k=1}^n \left(\frac{\partial^3 \eta_{kt}(c_t)}{\partial z_{kt}^2 \partial z_{l,t-1}} \cdot \mathbf{H}_{kit} \mathbf{H}_{kjt} + \frac{\partial^2 \eta_{kt}(c_t)}{\partial z_{kt} \partial z_{l,t-1}} \cdot \frac{\partial \mathbf{H}_{kit}}{\partial \hat{z}_{jt}} \right) \equiv 0, \quad (14)$$

where we have made use of the fact that entries of \mathbf{H}_t do not depend on $z_{l,t-1}$. Using different values r for c_t in Eq. (13) take the difference of this equation across them gives

$$\begin{aligned} &\frac{\partial^2 \log p(\hat{\mathbf{z}}_t | \hat{\mathbf{z}}_{t-1}; r+1)}{\partial \hat{z}_{it} \partial \hat{z}_{jt}} - \frac{\partial^2 \log p(\hat{\mathbf{z}}_t | \hat{\mathbf{z}}_{t-1}; r)}{\partial \hat{z}_{it} \partial \hat{z}_{jt}} \\ &= \sum_{k=1}^n \left[\left(\frac{\partial^2 \eta_{kt}(r+1)}{\partial z_{kt}^2} - \frac{\partial^2 \eta_{kt}(r)}{\partial z_{kt}^2} \right) \cdot \mathbf{H}_{kit} \mathbf{H}_{kjt} + \left(\frac{\partial \eta_{kt}(r+1)}{\partial z_{kt}} - \frac{\partial \eta_{kt}(r)}{\partial z_{kt}} \right) \cdot \frac{\partial \mathbf{H}_{kit}}{\partial \hat{z}_{jt}} \right] \equiv 0. \end{aligned} \quad (15)$$

If for any value of \mathbf{z}_t , $\mathbf{s}_{1t}, \hat{\mathbf{s}}_{1t}, \mathbf{s}_{2t}, \hat{\mathbf{s}}_{2t}, \dots, \mathbf{s}_{nt}, \hat{\mathbf{s}}_{nt}$ are linearly independent, to make the above equation hold true, one has to set $\mathbf{H}_{kit} \mathbf{H}_{kjt} = 0$ or $i \neq j$. That is, in each row of \mathbf{H}_t there is only one non-zero entry. Since h is invertible, then \mathbf{z}_t must be an invertible, component-wise transformation of a permuted version of $\hat{\mathbf{z}}_t$. \square

So far, the identifiability result has been established without observing the nonstationarity indicators such as domain indices.

A.3 Discussion on Assumptions in Theorem 2

This condition was initially introduced in GCL [11], namely, ‘‘sufficient variability’’, to extend the modulated exponential families [9] to general modulated distributions. Essentially, the condition says that the nonstationary domains c must have a sufficiently complex and diverse effect on the transition

distributions. In other words, if the underlying distributions are composed of relatively many domains of data, the condition generally holds true. Loosely speaking, the sufficient variability holds if the modulation of by c on the conditional distribution $q(z_{it} | \mathbf{z}_{\text{HX}}, c)$ is not too simple in the following sense:

1. Higher order of k ($k > 1$) is required. If $k = 1$, the sufficient variability cannot hold;
2. The modulation impacts λ_{ij} by \mathbf{u} must be linearly independent across domains c . The sufficient statistics functions q_{ij} cannot be all linear, i.e., we require higher-order statistics.

Further details of this example can be found in Appendix B of [11] and Appendix S1.4.1 of [18]. In summary, we need the domains denoted by c to have diverse (i.e., distinct influences) and complex impacts on the underlying data generation process.

In Theorem 1, we assume that the transition in latent space is in a Gaussian family, and then one may argue that the sufficient variability assumption cannot hold true. We can show that as long as the transition is not in the case that latents have additive Gaussian noise, the sufficient variability can still hold. The density of the latents can be expressed as:

$$p(z_{it} | \mathbf{z}_{t-1}, c_t) = \mathcal{N}(m(\mathbf{z}_{t-1}, c_t), \sigma(\mathbf{z}_{t-1}, c_t)). \quad (16)$$

Compared with the additive Gaussian noise case:

$$p(z_{it} | \mathbf{z}_{t-1}, c_t) = \mathcal{N}(m(\mathbf{z}_{t-1}, c_t), \sigma). \quad (17)$$

We can see that in additive Gaussian noise case the variance is a constant in terms of \mathbf{z}_t and \mathbf{z}_{t-1} . Then we write down the partial derivative of $\eta_{kt}(c_t)$ with respect to z_{kt} and $z_{l,t-1}$:

$$\frac{\partial \eta_{kt}^3(c_t)}{\partial z_{kt}^2 \partial z_{l,t-1}} = \frac{\partial \left(-\frac{1}{\sigma^2(\mathbf{z}_{t-1}, c_t)} \right)}{\partial z_{l,t-1}}. \quad (18)$$

If σ is constant in terms of $z_{l,t-1}$ which is always true in additive Gaussian noise case, then Eq. (18) is always zero, which violates the sufficient variability. However, if it is not additive Gaussian noise, in general Eq. (18) is non-zero. Then as long as the variance term changes sufficiently, the sufficient variability assumption holds.

B Implementation Details

B.1 Reproducibility

All experiments are done in a GPU workstation with CPU: Intel i7-13700K, GPU: NVIDIA RTX 4090, Memory: 128 GB. The code can be found via <https://github.com/xiangchensong/nctrl>.

B.2 Prior Likelihood Derivation

Let us start with an illustrative example of stationary latent causal processes consisting of two time-delayed latent variables, i.e., $\mathbf{z}_t = [z_{1,t}, z_{2,t}]$ with maximum time lag $L = 1$, i.e., $z_{i,t} = f_i(\mathbf{z}_{t-1}, \epsilon_{i,t})$ with mutually independent noises. Let us write this latent process as a transformation map \mathbf{f} (note that we overload the notation f for transition functions and for the transformation map):

$$\begin{bmatrix} z_{1,t-1} \\ z_{2,t-1} \\ z_{1,t} \\ z_{2,t} \end{bmatrix} = \mathbf{f} \left(\begin{bmatrix} z_{1,t-1} \\ z_{2,t-1} \\ \epsilon_{1,t} \\ \epsilon_{2,t} \end{bmatrix} \right). \quad (19)$$

By applying the change of variables formula to the map \mathbf{f} , we can evaluate the joint distribution of the latent variables $p(z_{1,t-1}, z_{2,t-1}, z_{1,t}, z_{2,t})$ as:

$$p(z_{1,t-1}, z_{2,t-1}, z_{1,t}, z_{2,t}) = p(z_{1,t-1}, z_{2,t-1}, \epsilon_{1,t}, \epsilon_{2,t}) / |\det \mathbf{J}_{\mathbf{f}}|, \quad (20)$$

where $\mathbf{J}_{\mathbf{f}}$ is the Jacobian matrix of the map \mathbf{f} , which is naturally a low-triangular matrix:

$$\mathbf{J}_{\mathbf{f}} = \begin{bmatrix} 1 & 0 & 0 & 0 \\ 0 & 1 & 0 & 0 \\ \frac{\partial z_{1,t}}{\partial z_{1,t-1}} & \frac{\partial z_{1,t}}{\partial z_{2,t-1}} & \frac{\partial z_{1,t}}{\partial \epsilon_{1,t}} & 0 \\ \frac{\partial z_{2,t}}{\partial z_{1,t-1}} & \frac{\partial z_{2,t}}{\partial z_{2,t-1}} & 0 & \frac{\partial z_{2,t}}{\partial \epsilon_{2,t}} \end{bmatrix}.$$

Given that this Jacobian is triangular, we can efficiently compute its determinant as $\prod_i \frac{\partial z_{i,t}}{\partial \epsilon_{i,t}}$. Furthermore, because the noise terms are mutually independent, and hence $\epsilon_{i,t} \perp \epsilon_{j,t}$ for $j \neq i$ and $\epsilon_t \perp \mathbf{z}_{t-1}$, we can write the RHS of Eq. 20 as:

$$\begin{aligned} p(z_{1,t-1}, z_{2,t-1}, z_{1,t}, z_{2,t}) &= p(z_{1,t-1}, z_{2,t-1}) \times p(\epsilon_{1,t}, \epsilon_{2,t}) / |\det \mathbf{J}_{\mathbf{f}}| \quad (\text{because } \epsilon_t \perp \mathbf{z}_{t-1}) \\ &= p(z_{1,t-1}, z_{2,t-1}) \times \prod_i p(\epsilon_{i,t}) / |\det \mathbf{J}_{\mathbf{f}}| \quad (\text{because } \epsilon_{1,t} \perp \epsilon_{2,t}) \end{aligned} \quad (21)$$

Finally, by canceling out the marginals of the lagged latent variables $p(z_{1,t-1}, z_{2,t-1})$ on both sides, we can evaluate the transition prior likelihood as:

$$p(z_{1,t}, z_{2,t} | z_{1,t-1}, z_{2,t-1}) = \prod_i p(\epsilon_{i,t}) / |\det \mathbf{J}_{\mathbf{f}}| = \prod_i p(\epsilon_{i,t}) \times |\det \mathbf{J}_{\mathbf{f}}^{-1}|. \quad (22)$$

Now we generalize this example and derive the prior likelihood below.

Let $\{f_i^{-1}\}_{i=1,2,3\dots}$ be a set of learned inverse transition functions that take the estimated latent causal variables, and output the noise terms, i.e., $\hat{\epsilon}_{i,t} = f_i^{-1}(\hat{z}_{i,t}, \{\hat{\mathbf{z}}_{t-\tau}, c_t\})$.

Design transformation $\mathbf{A} \rightarrow \mathbf{B}$ with low-triangular Jacobian as follows:

$$\underbrace{[\hat{\mathbf{z}}_{t-L}, \dots, \hat{\mathbf{z}}_{t-1}, \hat{\mathbf{z}}_t]^\top}_{\mathbf{A}} \text{ mapped to } \underbrace{[\hat{\mathbf{z}}_{t-L}, \dots, \hat{\mathbf{z}}_{t-1}, \hat{\epsilon}_{i,t}]^\top}_{\mathbf{B}}, \text{ with } \mathbf{J}_{\mathbf{A} \rightarrow \mathbf{B}} = \begin{pmatrix} \mathbb{I}_{nL} & 0 \\ * & \text{diag} \left(\frac{\partial f_{i,j}^{-1}}{\partial \hat{z}_{j,t}} \right) \end{pmatrix}. \quad (23)$$

Similar to Eq. 22, we can obtain the joint distribution of the estimated dynamics subspace as:

$$\log p(\mathbf{A}) = \log p(\hat{\mathbf{z}}_{t-L}, \dots, \hat{\mathbf{z}}_{t-1}) + \underbrace{\sum_{j=1}^n \log p(\hat{\epsilon}_{i,t}) + \log(|\det(\mathbf{J}_{\mathbf{A} \rightarrow \mathbf{B}})|)}_{\text{Because of mutually independent noise assumption}}. \quad (24)$$

$$\log p(\hat{\mathbf{z}}_t | \{\hat{\mathbf{z}}_{t-\tau}\}_{\tau=1}^L, c_t) = \sum_{j=1}^n \log p(\hat{\epsilon}_{i,t} | c_t) + \sum_{i=j}^n \log \left| \frac{\partial f_i^{-1}}{\partial \hat{z}_{i,t}} \right| \quad (25)$$

B.3 Derivation of ELBO

Then the second part is to maximize the Evidence Lower Bound (ELBO) for the VAE framework, which can be written as:

$$\begin{aligned} \text{ELBO} &\triangleq \log p_{\text{data}}(\mathbf{X}) - D_{KL}(q_\phi(\mathbf{Z}|\mathbf{X}) || p_{\text{data}}(\mathbf{Z}|\mathbf{X})) \\ &= \mathbb{E}_{\mathbf{Z} \sim q_\phi(\mathbf{Z}|\mathbf{X})} \log p_{\text{data}}(\mathbf{X}|\mathbf{Z}) - D_{KL}(q_\phi(\mathbf{Z}|\mathbf{X}) || p_{\text{data}}(\mathbf{Z}|\mathbf{X})) \\ &= \mathbb{E}_{\mathbf{Z} \sim q_\phi(\mathbf{Z}|\mathbf{X})} \log p_{\text{data}}(\mathbf{X}|\mathbf{Z}) - \mathbb{E}_{\mathbf{Z} \sim q_\phi(\mathbf{Z}|\mathbf{X})} [\log q_\phi(\mathbf{Z}|\mathbf{X}) - \log p_{\text{data}}(\mathbf{Z})] \\ &= \mathbb{E}_{\mathbf{Z} \sim q_\phi(\mathbf{Z}|\mathbf{X})} \left[\log p_{\text{data}}(\mathbf{X}|\mathbf{Z}) + \underbrace{\log p_{\text{data}}(\mathbf{Z})}_{\mathbb{E}_{\mathbf{c}}[\sum_{t=1}^T \log p(\mathbf{z}_t | \mathbf{z}_{t-1}, c_t)]} - \log q_\phi(\mathbf{Z}|\mathbf{X}) \right] \quad (26) \\ &= \mathbb{E}_{\mathbf{z}_t} \left[\underbrace{\sum_{t=1}^T \log p_{\text{data}}(\mathbf{x}_t | \mathbf{z}_t)}_{-\mathcal{L}_{\text{Recon}}} + \underbrace{\mathbb{E}_{\mathbf{c}} \left[\sum_{t=1}^T \log p_{\text{data}}(\mathbf{z}_t | \mathbf{z}_{t-1}, c_t) \right]}_{-\mathcal{L}_{\text{KLD}}} - \sum_{t=1}^T \log q_\phi(\mathbf{z}_t | \mathbf{x}_t) \right] \end{aligned}$$

B.4 Synthetic Dataset Generation

We generated two synthetic datasets (A and B) with different nonlinear mixing functions. In this section we will introduce the detailed implementation of the generation. The generation can be split into steps (1) sample c_t from a Markov chain, (2) generate \mathbf{z}_t with different transition functions f_{c_t} with respect to c_t , and (3) generate observation \mathbf{x}_t via mixing function \mathbf{g} .

B.4.1 Sample c_t from Markov chain

We first randomly initialized a Markov chain with transition matrix \mathbf{A} and sample 20,000 steps.

B.4.2 Generation of latent variables \mathbf{z}_t

We first randomly initialized $|C| = 5$ different transition functions $\{f_1, f_2, \dots, f_{|C|}\}$ with different MLPs, and generate $\mathbf{z}_t = f_{c_t}(\mathbf{z}_{\text{HX}})$. The dimensions are set to 8 for fair comparison.

B.4.3 Generation of observations \mathbf{x}_t

The difference between datasets A and B is the mixing function. We use a two-layer randomly initialized MLP for dataset A and a three-layer MLP for dataset B. For each linear layer in the MLP, we use condition number of the weight matrix to filter out ones that are not “invertible”.

B.5 Modified CartPole Dataset Generation

Similar to the synthetic datasets, we also sample from a Markov chain and get c_t . For the modified CartPole, we initialized 5 different environments which have different combinations of hyperparameters such as gravity, pole mass, etc. A detailed comparison is listed in Table 1.

Table 1: Different configs for different Modified CartPole environments.

Environment ID	Gravity	Pole Mass	Noise Scale
0	9.8	0.2	0.01
1	24.79	0.5	0.01
2	3.7	1.0	0.01
3	11.15	1.5	0.01
4	0.62	2.0	0.01

At each time step t the environment will load the corresponding hyperparameters for given c_t and update the states \mathbf{z}_t according to the configuration given c_t . The nonlinear mixing function from states to observations \mathbf{x}_t is fixed by a rendering method in the gym package.

B.6 MoSeq Dataset

In the MoSeq dataset, the observations \mathbf{x}_t are taken to be the first 10 principal components of depth camera video data of mice exploring an open field. The dataset consists of 20-minute depth camera recordings of 24 mice. In preprocessing, the videos are cropped and centered around the mouse centroid and then filtered to remove recording artifacts. Finally, the preprocessed video is projected onto the top principal components to obtain a 10-dimensional time series.

B.7 Mean Correlation Coefficient

MCC is a standard metric for evaluating the recovery of latent factors in ICA literature. MCC first calculates the absolute values of the correlation coefficient between every ground-truth factor against every estimated latent variable. Pearson correlation coefficients or Spearman’s rank correlation coefficients can be used depending on whether componentwise invertible nonlinearities exist in the recovered factors. The possible permutation is adjusted by solving a linear sum assignment problem in polynomial time on the computed correlation matrix.

B.8 Network Architecture

We summarize our network architecture below and describe it in detail in Table 2 and Table 3.

Table 2: Architecture details. BS: batch size, T: length of time series, i_dim: input dimension, z_dim: latent dimension, LeakyReLU: Leaky Rectified Linear Unit.

Configuration	Description	Output
ARHMM		
Autoregressive HMM for Synthetic Data		
Input: $\mathbf{x}_{1:T}$	Observed time series	$\text{BS} \times \text{T} \times \text{i_dim}$
Emission Module	Compute $\mu_{\mathbf{z}_{t+1}}, \sigma_{\mathbf{z}_{t+1}}$	$\text{BS} \times \text{T} \times 2 \times \text{z_dim}$
MLP-Encoder		
Encoder for Synthetic Data		
Input: $\mathbf{x}_{1:T}$	Observed time series	$\text{BS} \times \text{T} \times \text{i_dim}$
Dense	128 neurons, LeakyReLU	$\text{BS} \times \text{T} \times 128$
Dense	128 neurons, LeakyReLU	$\text{BS} \times \text{T} \times 128$
Dense	128 neurons, LeakyReLU	$\text{BS} \times \text{T} \times 128$
Dense	Temporal embeddings	$\text{BS} \times \text{T} \times \text{z_dim}$
MLP-Decoder		
Decoder for Synthetic Data		
Input: $\hat{\mathbf{z}}_{1:T}$	Sampled latent variables	$\text{BS} \times \text{T} \times \text{z_dim}$
Dense	128 neurons, LeakyReLU	$\text{BS} \times \text{T} \times 128$
Dense	128 neurons, LeakyReLU	$\text{BS} \times \text{T} \times 128$
Dense	i_dim neurons, reconstructed $\hat{\mathbf{x}}_{1:T}$	$\text{BS} \times \text{T} \times \text{i_dim}$
Factorized Inference Network		
Bidirectional Inference Network		
Input	Sequential embeddings	$\text{BS} \times \text{T} \times \text{z_dim}$
Bottleneck	Compute mean and variance of posterior	$\mu_{1:T}, \sigma_{1:T}$
Reparameterization	Sequential sampling	$\hat{\mathbf{z}}_{1:T}$
Prior Network		
Nonlinear Transition Prior Network		
Input	Sampled latent variable sequence $\hat{\mathbf{z}}_{1:T}$	$\text{BS} \times \text{T} \times \text{z_dim}$
InverseTransition	Compute estimated residuals $\hat{\epsilon}_{it}$	$\text{BS} \times \text{T} \times \text{z_dim}$
JacobianCompute	Compute $\log(\det(\mathbf{J}))$	BS

C Note on updated proof for identifiability of the nonstationary part

The original proof was based on the identifiability result of hidden Markov model in [20], in which the proof leverages the uniqueness of tensor decomposition from the three-way array in Kruskal’s method. In autoregressive version of the hidden Markov model, the construction of the three-way array is ill-defined. We modified the proof by leveraging the identifiability result in [21]. The authors thank Yingzhen Li and Carles Balsells-Rodas for pointing out this issue and helping to modify the proof.

Table 3: Architecture details on CNN encoder and decoder. BS: batch size, T: length of time series, h_dim: hidden dimension, z_dim: latent dimension, F: number of filters, (Leaky)ReLU: (Leaky) Rectified Linear Unit.

Configuration	Description	Output
CNN-Encoder	Feature Extractor	
Input: $\mathbf{x}_{1:T}$	RGB video frames	$BS \times T \times 3 \times 64 \times 64$
Conv2D	F: 32, BatchNorm2D, LeakyReLU	$BS \times T \times 32 \times 64 \times 64$
Conv2D	F: 32, BatchNorm2D, LeakyReLU	$BS \times T \times 32 \times 32 \times 32$
Conv2D	F: 32, BatchNorm2D, LeakyReLU	$BS \times T \times 32 \times 16 \times 16$
Conv2D	F: 64, BatchNorm2D, LeakyReLU	$BS \times T \times 64 \times 8 \times 8$
Conv2D	F: 64, BatchNorm2D, LeakyReLU	$BS \times T \times 64 \times 4 \times 4$
Conv2D	F: 128, BatchNorm2D, LeakyReLU	$BS \times T \times 128 \times 1 \times 1$
Dense	F: $2 * z_dim =$ dimension of hidden embedding	$BS \times T \times 2 * z_dim$
CNN-Decoder	Video Reconstruction	
Input: $\mathbf{z}_{1:T}$	Sampled latent variable sequence	$BS \times T \times z_dim$
Dense	F: 128, LeakyReLU	$BS \times T \times 128 \times 1 \times 1$
ConvTranspose2D	F: 64, BatchNorm2D, LeakyReLU	$BS \times T \times 64 \times 4 \times 4$
ConvTranspose2D	F: 64, BatchNorm2D, LeakyReLU	$BS \times T \times 64 \times 8 \times 8$
ConvTranspose2D	F: 32, BatchNorm2D, LeakyReLU	$BS \times T \times 32 \times 16 \times 16$
ConvTranspose2D	F: 32, BatchNorm2D, LeakyReLU	$BS \times T \times 32 \times 32 \times 32$
ConvTranspose2D	F: 32, BatchNorm2D, LeakyReLU	$BS \times T \times 32 \times 64 \times 64$
ConvTranspose2D	F: 3, estimated scene $\hat{\mathbf{x}}_{1:T}$	$BS \times T \times 3 \times 64 \times 64$